Inelastic scattering of molecules from a liquid polymer surface

J. Los, M. A. Gleeson, W. R. Koppers, T. L. Weeding, and A. W. Kleyn

Citation: The Journal of Chemical Physics **111**, 11080 (1999); doi: 10.1063/1.480466
View online: http://dx.doi.org/10.1063/1.480466
View Table of Contents: http://scitation.aip.org/content/aip/journal/jcp/111/24?ver=pdfcov
Published by the AIP Publishing

Inelastic scattering of molecules from a liquid polymer surface

J. Los, M. A. Gleeson, W. R. Koppers, T. L. Weeding, and A. W. Kleyn[a)]
FOM-Institute for Atomic and Molecular Physics, Kruislaan 407, 1098 SJ Amsterdam, The Netherlands

(Received 14 June 1999; accepted 28 September 1999)

The (dissociative) scattering of CF^+ and CF_2^+ ions from a perfluoropolyether is analyzed on the basis of the conservation laws of energy and momentum. The ion–surface collisions are treated as binary collisions between the primary ions and a representative group of the perfluoropolyether molecule. The energy partition between the two particles is analyzed on the basis of a statistical distribution between harmonic oscillators. The energy transfer between the individual atoms is treated as inelastic rovibrational excitation. This method not only allows us to draw some general conclusions concerning the dynamics of this type of molecule–surface collision, but also to estimate the dissociation probability of the scattered molecules as a function of the scattering angle and the energy loss. © *1999 American Institute of Physics.* [S0021-9606(99)70948-7]

I. INTRODUCTION

In the low and medium energy range (0.1–5 KeV), the scattering of atoms from solid surfaces is treated with considerable success in the framework of the single collision approximation.[1,2] In this approach the incident particle interacts with a ''free'' lattice atom, reducing the atom–surface interaction to a binary collision. Translational energy is transferred in the collision. The collisions are treated as purely elastic; inelastic effects such as internal energy uptake and electronic energy loss are neglected. In the single collision approximation, neglecting eventual inelastic processes, the scattering distribution can be calculated given the potential energy between the two colliding particles. Improvement of this description is gained by introducing the possibility of multiple collisions of the projectile with adjacent lattice atoms, which for example might explain rainbow features in the scattering profile. Finally, trajectory calculations, where the solid is represented by hundreds of lattice atoms, are now state of the art. The potential between the projectile and the lattice atoms, and between the lattice atoms mutually, is calculated applying the pair potential approximation.

The single collision approximation has been highly successful, mainly because in the energy range in which it is applied the unit cells are generally large with respect to the binary collision cross-sections. Moreover, most atom–surface scattering experiments are performed on a single crystalline surface, involving a highly ordered target. However, in the case of molecules scattering from an organic liquid polymer surface, the scattering process is much more complicated.[3–6] The bonding distances are much smaller, of the order of one angstrom. However, the distances between the molecular functional groups are larger. Instead of a highly ordered target we are dealing with molecules and ligands with specific shapes, and containing a variety of atoms,[7] which will not only serve as scattering centers, but also undergo vibrational excitation and even fragmentation.[8,9] The collisions can no longer be treated as purely elastic since inelastic effects, such as rotational and vibrational excitation of both the incident particle and the recoiling particle, can occur. To properly describe these kinds of collisions the internal energy uptake of the scattered and recoiling particles should be included.

Nevertheless, in two recent publications from our group[10,11] concerning, respectively, the scattering of CF_3^+, and of C^+, CF^+, and CF_2^+ from perfluoropolyethers (PFPE), it is shown that the binary collision approach is also reasonably successful in this case. In these experiments the angular and energy distributions of the scattered particles were measured. It appeared that, depending on the primary energy of the beam particles, substantial fragmentation took place. The main conclusions of this work are that the angular distributions indicate that the fragment particles are scattered off individual groups of the PFPE molecules and that in these collisions a large transfer of translational energy into vibrational energy is taking place. The analysis is based upon the binary elastic collision approximation, taking the average final energy of the fragments as the relevant parameter, yielding an effective target mass. From the independence of the degree of dissociation on the approach geometry it was concluded that single collisions prevail. In this paper we will analyze molecular scattering data, in particular that concerning CF^+, on the basis of the complete continuity relations.

II. EXPERIMENT

The experimental setup is described in detail in Ref. 12. Briefly, it consists of two UHV chambers. In one, the liquid sample can be characterized and stored. The sample can be transferred, under UHV, to a two-axis goniometer in the second chamber (base pressure of 1×10^{-10} mbar). The goniometer allows rotation of the target around an axis parallel to the surface to change the incoming angle θ_i (which is measured with respect to the surface normal), and around the surface normal to change the azimuthal angle. The total scattering angle θ is defined as $\theta=(180°-(\theta_i+\theta_f))$, where θ_f

a)Current address: Leiden Institute of Chemistry, Leiden University, Einsteinweg 55, P.O. Box 9502, 2300 RA Leiden, The Netherlands. Electronic-mail: a.kleyn@chem.leidenuniv.nl

FIG. 1. Schematic model of the PFPE molecule containing seven polymer subunits. The F, C, and O atoms are black, light gray, and white, respectively.

is the outgoing angle of the scattered particles (also defined with respect to the surface normal). A low-energy ion beamline, which produces the (fluoro)carbon ions, is mounted on the scattering chamber. The scattered ions are detected using a 90° cylindrical electrostatic energy analyzer with an energy resolution of $\Delta E/E \approx 0.08$. All energy spectra were measured in the scattering plane defined by the incident beam direction and the surface normal. The spectra shown throughout this paper have not been corrected for the energy-dependent transmission of the analyzer (proportional to E) to avoid an artificial enlargement of the intensities at very low energies. The detector can be rotated in the scattering plane from 45° to 180°, defined with respect to the incoming beam. The angular resolution of the detector is ~0.5°.

The liquid surface is supported on a stainless steel disc (diameter 10 mm, thickness 2 mm) that has been mechanically polished to a roughness below 0.05 μm. The disc is covered with a high molecular weight perfluoropolyether, sold under the trade name Krytox 16256. Its structural formula is given by $F[CF(CF_3)CF_2O]_{63(ave)}CF_2CF_3$. It has an average molecular weight of about 11 000 amu and a room temperature vapor pressure of $\sim 10^{-15}$ mbar. We obtained a smooth thin film by allowing the liquid to sheet across the stainless steel support. This could be done under UHV conditions by changing the azimuthal orientation. Figure 1 shows a schematic model of the polymer chain, containing seven of the polymer repeat units. The structure and composition of the surface produced by a supported film of this liquid has been the subject of a number of studies.[13–17] Beam scattering experiments using noble gas atoms point to hard-sphere-like collisions with $-CF_n$ $(n=1-3)$ groups protruding from the surface.[13,14] Reactive ion scattering measurements by Cooks and co-workers[15] suggest scattering from F and $-CF_3$ groups, while angle resolved photoelectron spectroscopy measurements by Pradeep and co-workers[16,17] demonstrate that the PFPE surface is predominantly formed by $-CF_3$ groups. All studies point to a surface structure in which the oxygen atoms are buried beneath the topmost layer. The molecule can achieve this by rearranging itself such that the $-CF_3$ side-groups and the end-groups form the outermost layer of the liquid, shielding the oxygen.

All spectra in this article were measured with a surface at room temperature. The PFPE film thickness was estimated to be of the order of 10 μm, ensuring that the possibility of the incident beam interacting with the metal support can be discounted. Although the layer is insulating, no evidence for charging was found even after prolonged beam exposure. Reproducible data could be obtained over several days. In addition, no changes in the spectra were observed as a result of changing the incoming particle flux. Only charged particles could be detected in our measurements. The neutralization efficiency is estimated to be ~90%.[10] The energy transfer involved in charge exchange is relatively small, and will not result in the scattered neutrals having a substantially different distribution. Hence, the analysis in this article should be applicable to all incident species, irrespective of their charge state. Fluorocarbon ions of mass greater than the mass of the primary particle (i.e., due to chemical pickup) are not observed, as confirmed by time-of-flight measurements.

III. RESULTS AND ANALYSIS

Some excellent reviews exist on classical scattering theory of atoms from solid surfaces.[1,2,18] We briefly review the most important equations and introduce an inelastic scattering component q in the binary elastic collision model.

A. Conservation of momentum and energy

In applying the laws of conservation to the scattering of CF_n^+ $(n=0-3)$ from a perfluoropolyether surface we assume that, in the energy range considered (50–200 eV), there is a representative molecular group that can be considered as ''free'' with respect to the environment. It is therefore sufficient to formulate the conservation laws for a binary collision between two molecules. We will indicate the projectile by the index 1 and the target by the index 2. We thus consider a binary inelastic collision of a primary particle having a mass M_1 and a translational energy before the collision $E_0 = 0.5 M_1 v_0^2$ with a surface particle of mass M_2 at rest. In this collision we do not neglect the internal energy uptake, i.e., vibrational and rotational energy, of the scattered products. The conservation laws of energy and momentum are given by

$$M_1 v_0 = M_1 v_1 \cos\theta + M_2 v_2 \cos\phi, \tag{1}$$

$$0 = -M_1 v_1 \sin\theta + M_2 v_2 \sin\phi, \tag{2}$$

$$0.5 M_1 v_0^2 = 0.5 M_1 v_1^2 + 0.5 M_2 v_2^2 + q. \tag{3}$$

The experimentally known parameters in these equations are M_1, the initial (v_0), and final (v_1) velocities of the projectile, and θ. We are presented with four unknown parameters in three equations. These are M_2, the final velocity of the target (v_2), the recoil angle of the target (ϕ), and the inelastic energy term (q). However, the expression for the final translational energy of the projectile as a function of θ,

$$\sqrt{E_1} = \frac{\cos\theta + \sqrt{A^2 - \sin^2\theta - A(1+A)Q}}{(A+1)}, \tag{4}$$

where $A = M_2/M_1$, gives us a means to determine M_2.

In Eq. (4), and in subsequent equations, we use reduced quantities for the energies. Thus, the final energies (E_1 and E_2) and the inelastic energy loss (Q) are reduced by E_0, the initial energy of the projectile; so

$$E_1 = \frac{0.5 M_1 v_1^2}{E_0}, \quad E_2 = \frac{0.5 M_2 v_2^2}{E_0}, \quad \text{and} \quad Q = \frac{q}{E_0}.$$

Hence, only E_0 has units and the remaining quantities are unitless. Now neglecting the possibility of superelastic colli-

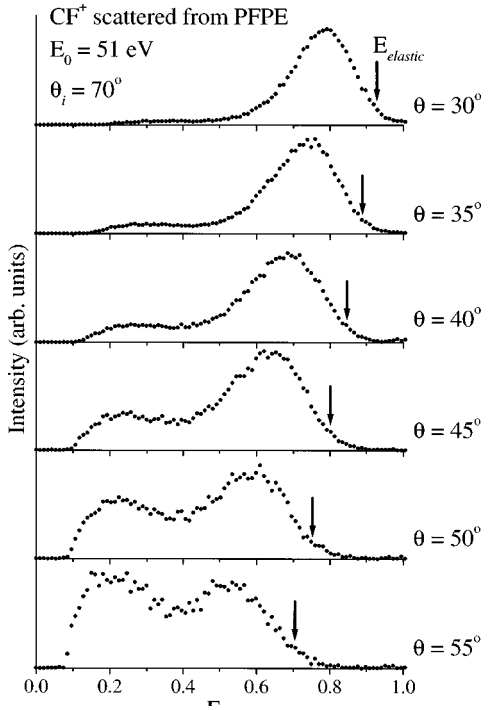

FIG. 2. The intensity of the cations scattered from PFPE as a function of the relative final energy E_1 for 51 eV CF^+ molecules incident at $\theta_i=70°$. The low E_1 peak is mainly due to C^+, while the high E_1 peak is predominantly CF^+. The scattering angle is varied in steps of 5° from $\theta=30°$ to $\theta=55°$. The arrows indicate the value of E_1 assigned for elastic scattering ($Q=0$).

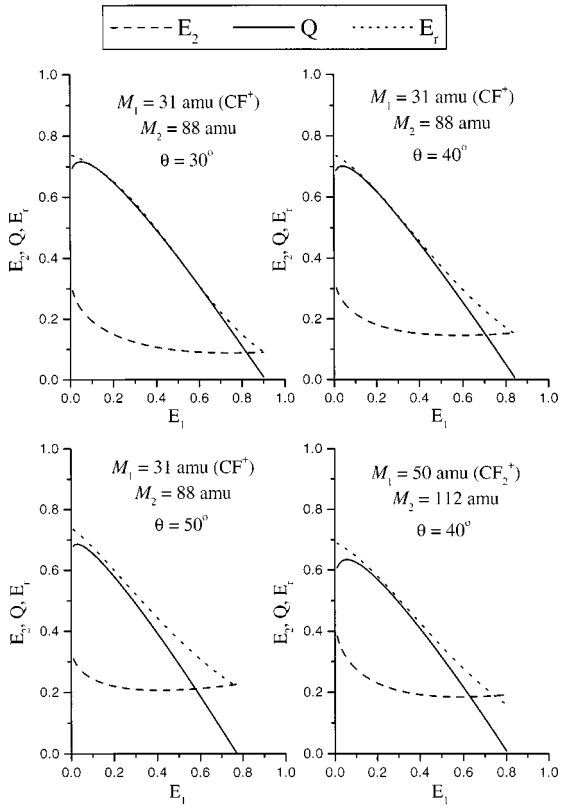

FIG. 3. The relative energies E_2, Q, and E_r as a function of E_1 for CF^+ (a), (b), (c) and for CF_2^+ (d) scattered from PFPE. For CF^+ the mass ratio is $A=2.84$ and for CF_2^+ $A=2.24$. For CF^+ the scattering angle is varied in steps of 10° from $\theta=30°$ to $\theta=50°$. For CF_2^+, $\theta=40°$.

sions, the upper bound of the energy distribution, for a given M_2 at a particular scattering angle, is given by Eq. (4) when $Q=0$.

In Fig. 2 we show a set of measurements concerning the scattering of CF^+. The primary energy is 51 eV and the angle of incidence with respect to the surface normal is 70°. The arrows indicate the position on the energy scale that we have assigned for $Q=0$. Because the resolution of the energy analyzer is $\Delta E/E\approx 0.08$, the arrows on the energy scale (E_{elastic}) are chosen such that the intensity of the scattered CF^+ peak reduces to zero at $E\approx 1.08E_{\text{elastic}}$ (i.e., E_{elastic} is assigned solely on the basis of the measured intensity and the analyzer resolution). The arrows on Fig. 2 correspond to a value for M_2 of ~ 88 amu. Note that, although the E_{elastic} arrow is assigned independently for each valve of θ, the same value for M_2 is obtained in all cases. It should be remarked that we differ here from the analysis of Koppers *et al.*,[10–12] who took the parent ion maximum in the energy distributions for the determination of the mass of the target molecule, and hence obtained a smaller M_2 for CF^+ scattering.[11] In that case M_2 was not constant as a function of θ. We will return to this point in the last section, in particular to the question of why the maximum is located at energies lower than the elastic scattering energy.

The value of M_2 (the mass of the ''free'' molecular group in the collision with the projectile) determines how, at a certain scattering angle θ and final energy E_1, the energy loss $(1-E_1)$ is divided between translational energy E_2 and inelastic energy Q. The value of M_2 is quite sensitive to the value of E_1 that is selected as corresponding to $Q=0$. As an illustration of this for a projectile ($M_1=31$ amu) scattered elastically through $\theta=40°$, final values for E_1 of 0.807, 0.846, and 0.864 correspond to values for M_2 of 69, 88, and 100 amu, respectively. The value of M_2 has an influence on Figs. 3 and 7 in this paper, however this influence is not substantial. Figure 2 shows that a single mass M_2, which holds over a range of scattering angles, can be assigned to the surface, consistent with a surface comprised of uniform functional groups as proposed.[15–17] Now given M_2 we can calculate E_2, Q, and ϕ. However, first we will discuss the limits between which Q is confined. It is well known that in the collision between a moving particle (mass M_1) and a stationary particle (mass M_2), the initial relative energy E_{rel} is given by

$$E_{\text{rel}}=\frac{M_2}{M_1+M_2}=\frac{A}{A+1}, \tag{5}$$

while the center-of-mass energy is

$$E_{\text{cm}}=\frac{M_1}{M_1+M_2}=\frac{1}{A+1} \tag{6}$$

times the primary energy, E_0. E_{rel} is the maximum energy that is available for internal excitation in a biparticle collision (i.e., E_{rel} is the maximum of Q). However, this maximum is only reached in a headon collision in which the two particles recombine. In cases where the projectile is scattered

over a certain angle, the conservation of momentum puts more restrictions on the transfer of primary energy to internal modes. One of these limits can be obtained by the expression for E_2:

$$\sqrt{E_2}=\frac{\sqrt{A}\cos\phi\pm\sqrt{A\cos^2\phi-(A+1)Q}}{(A+1)}. \tag{7}$$

Since $(A\cos^2\phi-(A+1)Q)\geqslant 0$ we obtain for the upper bound of Q

$$Q\leqslant\frac{A}{A+1}\cos^2\phi=E_r. \tag{8}$$

A similar relationship in terms of θ can be obtained from Eq. (4), but in our case that is only of importance for very small values of E_1.

To express the three unknown quantities E_2, Q, and ϕ in terms of the experimentally determined E_1 and θ, several routes can be followed. Providing perhaps the best insight into the dependencies are the following:

$$E_2=\frac{1}{A}(1-2\sqrt{E_1}\cos\theta+E_1), \tag{9}$$

$$Q=1-E_1-E_2, \tag{10}$$

$$E_r=\frac{A}{A+1}\cos^2\phi=\frac{A}{A+1}\frac{(1-\sqrt{E_1}\cos\theta)^2}{AE_2}. \tag{11}$$

Equation (9) clearly shows the behavior of E_2 as a function of the various quantities: it is inversely proportional to the mass ratio A; it increases with increasing scattering angle θ, and it is only slightly dependent on the final energy of the scattered particle E_1. Combined with the conservation of energy it shows that for a fixed θ and E_1, the partition of energy over E_2 and Q is determined by A.

Here a remark on the interpretation of the continuity equations is appropriate. As is clear from Eq. (10), when measuring the E_1 energy distribution at a certain angle θ, the sum of Q and E_2 is determined as a function of E_1. By choosing a certain value for the mass of the target (M_2), values for Q and E_2 are obtained. In this study we determined M_2, and thus A from the outer edge of the energy distribution, taking into account the full width at half maximum (FWHM) of the energy analysis. If this point in the energy distribution is only reached in a multiple collision (let us suppose the particle has two identical collisions on two adjacent CF_3 groups) then the value obtained for M_2, which is assigned under the assumption of a single collision, will be substantially larger than (almost twice) the mass of a CF_3 group. Furthermore, the value assigned to M_2 will not be constant as a function of θ if a double collision process is treated as a single collision. In this case a single collision on a CF_3 group would be considered as inelastic, the inelastic energy being due to the relative motion of the two neighboring CF_3 groups. In this experiment, in particular for the CF^+ measurements, it is clear that multiple collisions play a negligible role, since we find a value for M_2 that is close to 69 and constant as a function of θ. A multiple collision would in this description appear to be a superelastic collision ($E_1 > E_{\text{elastic}}$).

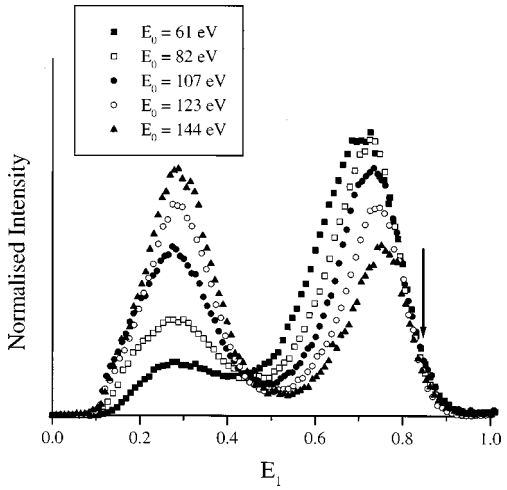

FIG. 4. The area normalized intensity of the cations scattered from PFPE as a function of the relative final energy E_1 for incident CF^+ molecules. The low E_1 peak is mainly due to C^+, while the high E_1 peak is predominantly CF^+. The angle of incidence with respect to the surface normal $\theta_i=70°$ and the scattering angle is $\theta=40°$. The primary energy E_0 is varied from 61 to 144 eV. The arrow indicates the value of E_1 assigned for elastic scattering ($Q=0$) (mass ratio $A=2.84$).

In Fig. 3 we show for CF^+ a set of graphs representing E_2 (dashed), Q (solid), and E_r (dotted) as a function of E_1 for three different scattering angles $\theta=30°$, 40°, and 50° [(a), (b), and (c) respectively]. Figure 3(d) is for CF_2^+ at scattering angle of $\theta=40°$. These figures relate to values of A ($M_2=88$ for CF^+, and $M_2=112$ for CF_2^+) that have been determined from the upper bound of the energy distributions as illustrated for CF^+ in Fig. 1. Although the validity of the laws of conservation over the domain of E_1 cannot be questioned, it might be an advantage, in particular for $E_1\ll 1$, to introduce in the kinetic analyses of these collisions the complexity of both projectile and target.

B. Energy partitioning

In Fig. 2 we observe that the energy distribution of the scattered ions has two maxima. Koppers *et al.*[11] show that these maxima can be identified with, respectively, CF^+ parent ions and C^+ fragment ions. The assumption made is that upon dissociation of CF^+ to C^+ and F the kinetic energy release is small with respect to the final energy of the fragments. As the fragmentation is caused by vibrational excitation this assumption is very reasonable and will be discussed later. Furthermore we observe in Fig. 2 that at higher scattering angles the degree of dissociation increases. Qualitatively this can be explained with the help of Fig. 3. At a scattering angle $\theta=30°$ the maximum of the CF^+ peak lies at $E_1\approx 0.8$, while for $\theta=50°$ this maximum is found at $E_1\approx 0.6$. At these positions on the E_1 scale, the reduced inelastic energy Q increases by a factor of ~ 2 when θ is changed from 30° to 50°, resulting in increased fragmentation.

In order to investigate this effect in a more quantitative way we show in Fig. 4 a set of measurements concerning the energy distribution of the CF^+ ions scattered at a fixed angle $\theta=40°$. The initial energies range from $E_0=61$ to 144 eV. The E_1 curves are mutually normalized to the same area

underneath the curve and they are superimposed on each other using the same abscissa. This way of displaying the data is very instructive. In the first place we see that our method of determining the mass of the fluid molecule M_2, which takes the load of the momentum and energy transfer in the collision, remains valid as a function of E_0. Since for a rovibrational excitation the average inelastic energy loss is proportional to the primary energy E_0, a plot of the ion intensity of the scattered particles as a function of the reduced energy E_1 for a range of primary energies should result in identical curves. So the experimental curves should overlap at and around the point of the E_1 curves where the scattering is elastic or near-elastic, i.e., as is the case at $E_1 \sim 0.846$. Elastic scattered particles can be observed above the arrow because of the limited resolution of the energy analyzer. Below the arrow, down to $E_1 \approx 0.8$, near-elastic scattered particles are observed. The real inelastic energy, even at the highest primary energy of 144 eV, only amounts to ~ 6.6 eV at $E_1 = 0.8$. This inelastic energy is shared between the target and the projectile, so the energy stored in the projectile will be about 3 eV, close to the amount needed for dissociation of CF^+.[11] In contrast, assigning M_2 on the basis of the CF^+ peak maximum would result in its value increasing with E_0. As noted for Fig. 1, M_2 will also increases with increasing θ for constant E_0 if its determination is based on the position of the peak maximum. This is a consequence of an increase in either E_0 or θ resulting in an increase in the inelastic energy (q) available at a given E_1. The absolute increase in q is greater at lower E_1. Hence, as either parameter increases molecules with lower E_1 dissociate preferentially, resulting in a shift of the peak maximum to higher E_1 and an apparent increase in M_2. Second, we observe that the relative intensity of the CF^+ peak is decreasing with increasing E_0. This is balanced by the relative increase of the C^+ signal. However, it is also clear that the E_1-distributions cannot be unequivocally divided into a CF^+ part and a C^+ part.

In order to test the assumption that the dissociation takes place at threshold (i.e., that the kinetic energy release can be neglected) we have to chose carefully an interval on the E_1 scale where we can compare the intensity of a pure C^+ signal with a pure CF^+ signal. Given the fact that for $E_1 \leqslant 0.1$ no scattered ions are observed, we may be sure that no CF^+ ions are measured for $E_1 < 0.258$. This boundary is given by the fact that the energy ratio between a parent ion and a fragment ion of the same velocity equals their mass ratio (i.e., ~ 2.58 for CF^+ and C^+). Thus, the interval of $0.1 < E_1 < 0.258$ consists solely of C^+ ions. This corresponds with an interval of $0.258 < E_1 < 0.667$ for CF^+. However, in the lower part of this interval the CF^+ signal may be contaminated by C^+ ions originating from dissociation of CF^+ with $E_1 > 0.667$. Hence, we restrict ourselves to an interval $0.52 < E_1 < 0.78$ for the CF^+ ion signal, and related to that the interval $0.2 < E_1 < 0.3$ for determining the C^+ ion signal. However, as will be seen, for $E_1 > 0.27$ the intensity is a mixture of C^+ and CF^+.

In Fig. 5 we show the result of adding the ion signal in the interval 0.2–0.3 (I_{C^+}) to the ion signal in the interval 0.52–0.78 (I_{CF^+}). Prior to this addition a single three-point smoothing was applied to data shown in Fig. 4. The energy spectra are not corrected for the energy transmission of the analyzer. This is correct since in the dissociation of CF^+ to C^+ (+F) not only is the nominal value of E_1 for the C^+ fragment reduced by a factor of 2.58, but also ΔE_1. From Fig. 5 it is obvious that for $E_1 \leqslant 0.7$ the measurements taken at different primary energies converge to a uniform curve. Above that value this is no longer the case due to ion mixing. Hence the assumption of dissociation of CF^+ at threshold is verified for the regions associated with a single scattered species. The uniformity of the curves across the range of primary energies also demonstrates the absence of preferential neutralization of one of the scattered ions. In contrast, we note that in the case of scattering of CF_3^+ from metals charge transfer effects dominate.[19–22]

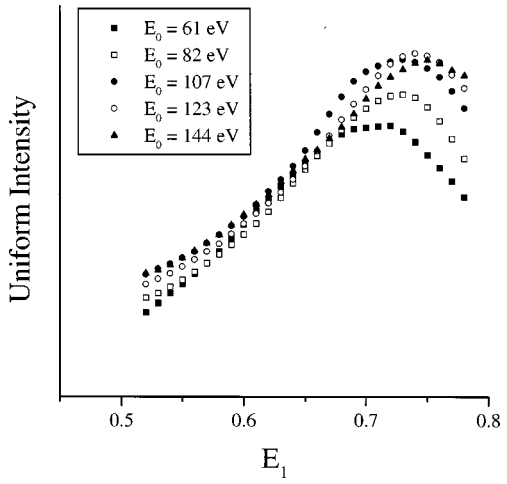

FIG. 5. The energy distributions of Fig. 4 from $E_1 = 0.52$ to $E_1 = 0.78$, to which are added the corresponding C^+ contributions (see text).

Figure 6 now gives the dissociation probability of the scattered CF^+ molecules ($I_{C^+}/(I_{C^+} + I_{CF^+})$) as a function of E_1 in the interval under consideration. Again we observe a systematic trend up to $E_1 \sim 0.7$. All curves are decreasing almost linearly with increasing E_1. Referring again to Fig. 3, the reduced inelastic energy component is decreasing almost linearly in this range. Furthermore, since the actual inelastic energy corresponds to $q = Q \times E_0$, we expect a higher dissociation probability at higher primary energy, as is seen.

Finally in Fig. 7 we show the natural logarithm of the dissociation probability as a function of the inverse of $E_r \times E_0$. Points that deviated strongly from the general trend shown in Fig. 6 ($E_1 \geqslant 0.7$) have been excluded from Fig. 7. In the allowed interval all points converge to a uniform line. This way of representing the data is inspired by the treatment of Forst[23] on the ''energy partitioning among fragments'' that results from the dissociation of a super excited molecule. His simplifying assumptions are that the molecule consists of a number of degenerate harmonic oscillators, and that the energy partitioning among the fragments is purely statistical. Supposing now that n quanta of energy have to be divided among two harmonic oscillators, a and b, which are p_a- and p_b-fold degenerate, Forst derives that the normalized probability to find n_a quanta in oscillator a, $P(n_a, n)$, is given by

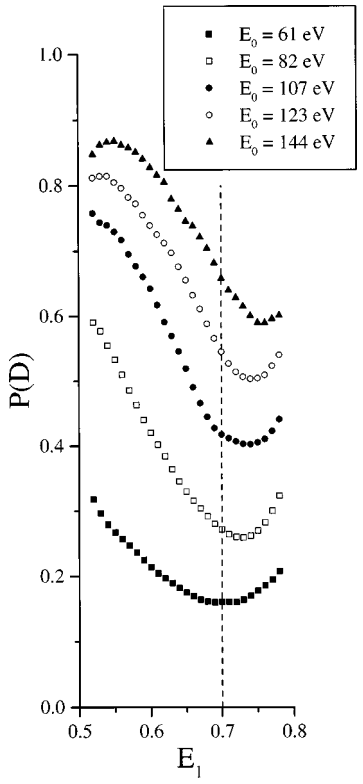

FIG. 6. The dissociation probability of CF^+ $(I_{C^+}/(I_{C^+}+I_{CF^+}))$ scattered from PFPE in the energy domains $0.52 \leqslant E_1 \leqslant 0.78$. The data used are from Fig. 4.

$$P(n_a,n)=\frac{(n_a+p_a-1)!}{n_a!(p_a-1)!}\times\frac{(n-n_a+p_b-1)!}{(n-n_a)!(p_b-1)!}\times\frac{n!(p-1)!}{(n+p-1)!}, \tag{12}$$

with $p=p_a+p_b$.

Given the fact that in our case CF^+ is a single oscillator; $p_a=1$ and $P(n_a,n)$ reduces to

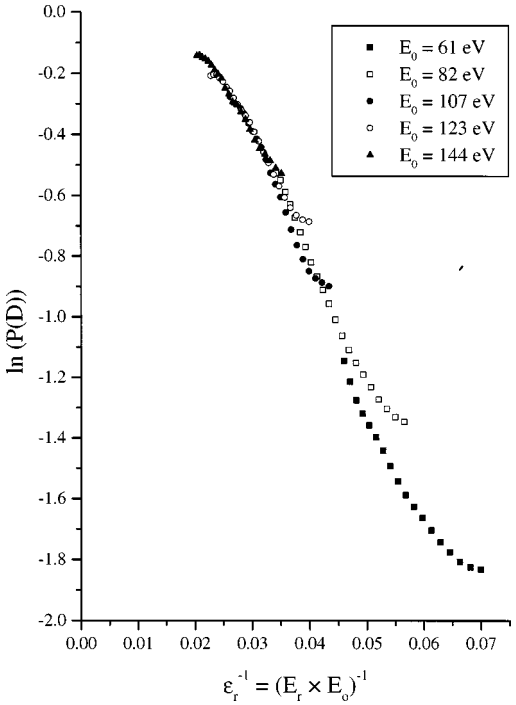

FIG. 7. The natural logarithm of the dissociation probabilities shown in Fig. 6 as a function of $(E_r\times E_0)^{-1}$, the inverse of the energy available in the collision for dissociation.

$$P(n_a,n)=(p-1)\frac{(n-n_a+p-2)!}{(n-n_a)!}\times\frac{n!}{(n+p-1)!}. \tag{13}$$

If the number of quanta needed to dissociate the CF^+ molecule is n_d, then the probability for dissociation, $P(D)$, is obtained by summing up $P_{(n_a,n)}$ over n_a from $n_a=n_d$ to $n_a=n$. Making use of the recurrence relation

$$(p-1)\frac{(n-n_a+p-2)!}{(n-n_a)!}=-\frac{(n-(n_a+1)+p-1)!}{(n-(n_a+1))!}+\frac{(n-n_a+p-1)!}{(n-n_a)!}, \tag{14}$$

we obtain

$$P(D)=\frac{n!}{(n+p-1)!}\times\frac{(n-n_d+p-1)!}{(n-n_d)!}=\frac{(n-n_d+1)(n-n_d+2)\cdots(n-n_d+p-2)(n-n_d+p-1)}{(n+1)(n+2)\cdots(n+p-2)(n+p-1)}. \tag{15}$$

Now, assuming $p \ll n$ and n_d, then

$$P(D)\approx\left(1-\frac{n_d}{n}\right)^{p-1}. \tag{16}$$

The number of quanta required to dissociate the CF^+ molecule (n_d) is proportional to the dissociation energy (D) while n is proportional to the energy that is available in a specific collision for internal excitation, $\epsilon_r=E_0\times E_r$. Hence

$$P(D)\approx(1-D\epsilon_r^{-1})^{p-1}. \tag{17}$$

In our experiment $D \ll \epsilon_r$. Thus the logarithm of $P(D)$ is approximated by

$$\ln P(D)\approx(p-1)\ln(1-D\epsilon_r^{-1})\approx-(p-1)D\epsilon_r^{-1}. \tag{18}$$

Therefore, from a plot of the logarithm of $P(D)$ as a function of ϵ_r^{-1}, as is shown in Fig. 7, the approximate value for the product $(p-1)D$ can be determined as a function of the inverse of ϵ_r.

It is clear that if the product $(p-1)D$ is constant, then the logarithm plot of $P(D)$ would approximately yield a straight line that goes through the origin. Figure 7 shows that this definitely is not the case. Since the dissociation energy (D) does not depend on the primary energy (E_0) of the CF^+ molecules, it can be concluded that $(p-1)$, the sum of the degrees of freedom of the colliding molecules, is a function of E_r. A theoretical value for the dissociation of CF^+, $D=7.4\,\text{eV}$, has been derived by O'Hare and Wahl.[24] However, CF^+ is formed by electron impact on CF_4 and therefore will be vibrationally excited. Koppers *et al.*[11] determined, from a measurement of the average internal energy as a function of the energy loss of the scattered particle, that the average internal energy of the CF^+ molecules in the primary beam is $\sim 4.5\,\text{eV}$. So the energy required to dissociate CF^+ is 3 eV. Substituting this value into Eq. (18), we find $(p-1)\approx 2$ for $\epsilon_r^{-1}=0.02$ (the highest energy loss). $(p-1)$ rises as a function of ϵ_r^{-1} to a value of $(p-1)\approx 9$ for $\epsilon_r^{-1}=0.05-0.07$. $(p-1)$ corresponds to the number of degrees of freedom of the group from which the CF^+ is scattered (the CF^+ being considered as having 1 degree of freedom). This strongly suggests that in soft collisions corresponding with a large impact parameter, CF^+ interacts with the CF_3 surface group as a whole, the inelastic energy being stored in about 9 degrees of freedom. However, for hard collisions corresponding with a small impact parameter the interaction is primarily with part of the CF_3 surface group, say CF. The inelastic energy is then deposited in the local CF vibrational mode, and in the relative motion between the CF and the remainder of the surface group, two degrees of freedom. So the energy transfer to CF in such a hard collision is shared by this vibrational excitation and the translational energy of the center-of-mass of the CF_3 surface group. This is in agreement with our kinematic analysis, which is based upon the assumption that CF^+ is scattered from an ''isolated'' functional group at the surface.

Finally, if we accept that the PFPE surface is predominantly composed of CF_3 groups and taking the premise that the CF^+ scatters from a single, isolated molecule on the surface, then the mass of $M_2=88$ requires that molecule to have a minimum of four bonds (five atoms). This is entirely consistent with a value of $(p-1)=9$. This molecule can be envisaged as a CF_3 (mass 69) group with the PFPE polymer chain, acting as a single group, providing the remainder of the effective mass (we will denote this group as CF_3 poly).

Notwithstanding the surprising numerical results of these considerations on the energy partitioning among the colliding molecules, some care is needed. In the first place there are the unavoidable errors in the determination of the degree of dissociation of CF^+ from five separate measurements, in particular at the lowest primary energy, where the degree of dissociation is small. To estimate these errors is difficult. Secondly, the treatment of Forst[23] concerns the dissociation of an energy-rich molecule, while in this case it is assumed that in the collision a collision complex is formed with an energy content equal to ϵ_r, the amount of energy available for partitioning among the different degrees of freedom.

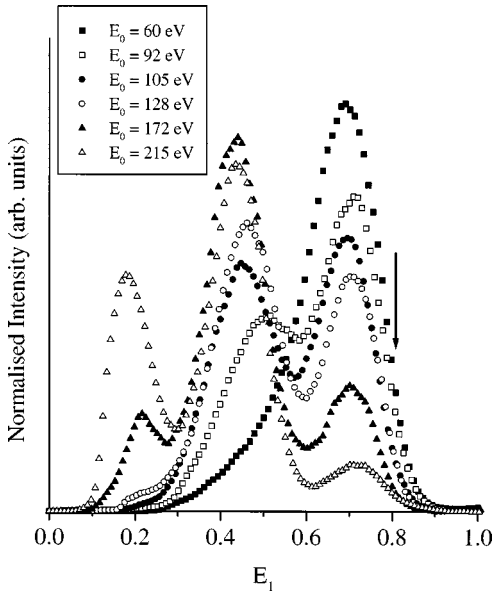

FIG. 8. The area normalized intensities of cations scattered from PFPE as a function of the relative final energy E_1 for incident CF_2^+ molecules. The peaks correspond to scattered C^+ (low E_1), CF^+, and CF_2^+ (high E_1), respectively. The angle of incidence with respect to the surface normal $\theta_i=70°$ and the scattering angle is $\theta=40°$. The primary energy E_0 is varied between 60 and 215 eV. The arrow indicates the value of E_1 assigned for elastic scattering $(Q=0)$ (mass ratio $A=2.24$).

IV. DISCUSSION AND CONCLUSIONS

From Fig. 3 we deduce that, for a given mass ratio A there is a unique relationship between the final energy of the scattered particle (E_1) and Q. Since both quantities are reduced with respect to the primary energy E_0, this relationship is independent of E_0. Now in Fig. 5 we see that over the experimental energy range considered the E_1-curves converge to a single uniform shape. This means that the inelastic energy in the collisions is due to rovibrational excitation, as only this type of excitation is proportional to the primary energy: no electronic energy is involved.

The main advantage of applying the complete conservation laws in analyzing experimental scattering data lies in the possibility of relating the final energy of the scattered particle in a systematic and consistent procedure to the inelastic energy deposited in the colliding particles. This gives the opportunity to obtain from this type of experiment quite accurate data about the fragmentation of molecules, e.g., binding energies and structural composition. To this end it will be necessary to measure simultaneously the energy and the mass of the scattered particles. This is illustrated by Fig. 8, which shows a set of data on CF_2^+, taken at a scattering angle of 40°. We see a gradual rise of the CF^+ signal and, at higher energies, of the CF^+ signal as a function of E_0. The fragmentation sequence probably proceeds stepwise $CF_2^+ \rightarrow CF^+ + F \rightarrow C^+ + F + F$, similar to metals.[21] Direct fragmentation to the final product C^+ is less likely. Although it is very tempting to proceed as in the case of CF^+, this is not possible because the energy distributions of the different masses overlap too much.

It should be stressed once again that the conservation laws only give relationships between several physical quan-

tities. To describe the scattering distribution, and thus the dynamics of scattering processes, a model is needed. Nevertheless some conclusions can be drawn, in particular from the energy distribution as a function of the scattering angle. As already explained, the mass ratio A can be obtained from the rising edge of the E_1 distribution. Considering now the CF^+ curves of Figs. 4 and 5, we see that the maximum of the E_1 distribution lies at a value $E_1=0.7$, about 0.15 lower than the elastic scattering position. This should be due to a steric effect causing, for most orientations of the CF^+ molecule at the point of impact, a strong rotational excitation, which is proportional to E_0. Comparing with this behavior, we see in figure 8 that in the scattering of CF_2^+ the dissociation starts much earlier than for CF^+ (the peak maximum is ~ 0.1 below the elastic scattering position). This is probably due to the fact that the steric effect in CF_2^+ causes an efficient excitation of the low frequency bending mode followed by dissociation.

In the case of both CF^+ and CF_2^+ we observe from the energy distributions that below the peak maxima there are low intensity tails that go at particular values of E_1 to zero. For CF^+ we see that the CF^+ threshold lies at $E_1=0.1$ and, correcting for the mass effect, the threshold of CF^+ lies at $E_1=0.258$. For CF_2^+ the threshold of the parent peak lies at $E_1=0.333$. This behavior indicates that at high values of E_1 the collision ''probes'' the whole mass of the target molecule, which will be the case at relatively large impact parameter. At lower values of E_1 on the other hand, the interaction will take place predominantly with one or two atoms of the target resulting in a kind of spectator model. Indeed, a real spectator- like interaction will lead to a ''forbidden'' region in the E_1 distribution, depending on the scattering angle. These conclusions are strongly sustained by the results of the measurements on the dissociation probability. In soft collisions CF^+ interacts with the CF_3 poly group of the PFPE molecule (i.e., the side- or end-group of the PFPE with some contribution from the polymer chain). In hard collisions the inelastic scattering is determined by a CF^+–CF interaction.

ACKNOWLEDGMENTS

The authors would like to thank F.G. Giskes and R. Schaafsma for technical support. This work is part of the research program of the Stichting voor Fundamenteel Onderzoek der Materie (FOM), which is financially supported by the Nederlandse Organisatie voor Wetenschappelijke Onderzoek (NWO).

[1] S. R. Kasi, H. Kang, C. S. Sass, and J. W. Rabalais, Surf. Sci. Rep. **10**, 1 (1989), and references therein.
[2] H. Niehus, W. Heiland, and E. Taglauer, Surf. Sci. Rep. **17**, 213 (1993), and references therein.
[3] G. M. Nathanson, P. Davidovits, D. R. Worsnop, and C. E. Kolb, J. Phys. Chem. **100**, 13007 (1996).
[4] S. B. Wainhaus, H. Lim, D. G. Schultz, and L. Hanley, J. Chem. Phys. **106**, 10329 (1997).
[5] D. G. Schultz, S. B. Wainhaus, L. Hanley, P. de Sainte Claire, and W. L. Hase, J. Chem. Phys. **106**, 10337 (1997).
[6] S. B. M. Bosio and W. L. Hase, Int. J. Mass Spectrom. Ion Processes **174**, 1 (1998).
[7] J. G. Harris, J. Phys. Chem. **96**, 5077 (1992).
[8] I. Benjamin, M. Wilson, and A. Pohorille, J. Chem. Phys. **100**, 6500 (1994).
[9] N. Lipkin, R. B. Gerber, N. Moiseyev, and G. M. Nathanson, J. Chem. Phys. **100**, 8408 (1994).
[10] W. R. Koppers, J. H. M. Beijersbergen, T. L. Weeding, P. G. Kistemaker, and A. W. Kleyn, J. Chem. Phys. **107**, 10736 (1997).
[11] W. R. Koppers, M. A. Gleeson, J. Lourenço, T. L. Weeding, J. Los, and A. W. Kleyn, J. Chem. Phys. **110**, 2588 (1999).
[12] W. R. Koppers, Ph.D. thesis, University of Amsterdam, 1997.
[13] M. E. King, G. M. Nathanson, M. A. Hanning-Lee, and T. K. Minton, Phys. Rev. Lett. **70**, 1026 (1993).
[14] M. E. King, M. E. Saecker, and G. M. Nathanson, J. Chem. Phys. **101**, 2539 (1994).
[15] T. Pradeep, S. A. Miller, H. W. Rohrs, B. Feng, and R. G. Cooks, Mater. Res. Soc. Symp. Proc. **380**, 93 (1995).
[16] T. Pradeep, Chem. Phys. Lett. **243**, 125 (1995).
[17] S. Ramasamy and T. Pradeep, J. Chem. Phys. **103**, 485 (1995).
[18] *Low Energy Ion-Surface Interactions*, edited by J. W. Rabalais (Wiley, UK, 1994).
[19] W. R. Koppers, J. H. M. Beijersbergen, K. Tsumori, T. L. Weeding, P. G. Kistemaker, and A. W. Kleyn, Phys. Rev. B **53**, 11207 (1996).
[20] W. R. Koppers, J. H. M. Beijersbergen, K. Tsumori, T. L. Weeding, P. G. Kistemaker, and A. W. Kleyn, Surf. Sci. **357–358**, 678 (1996).
[21] W. R. Koppers, J. H. M. Beijersbergen, K. Tsumori, T. L. Weeding, P. G. Kistemaker, and A. W. Kleyn, Int. J. Mass Spectrom. Ion Processes **174**, 11 (1998).
[22] R. G. Cooks, T. Ast and M. A. Mabud, Int. J. Mass Spectrom. Ion Processes **100**, 209 (1990), and references therein.
[23] *Theory of Unimolecular Reactions*, edited by W. Forst (Academic, New York, 1973), pp. 269–273.
[24] P. A. G. O'Hare and A. C. Wahl, J. Chem. Phys. **55**, 666 (1971).